

Pedestrian, Crowd, and Evacuation Dynamics

Dirk Helbing^{1,2} and Anders Johansson¹

¹ Dresden University of Technology, Andreas-Schubert-Str. 23, 01062 Dresden, Germany

² Collegium Budapest – Institute for Advanced Study, Szentháromság utca 2, 1014 Budapest, Hungary

1 Article Outline

This contribution describes efforts to model the behavior of individual pedestrians and their interactions in crowds, which generate certain kinds of self-organized patterns of motion. Moreover, this article focusses on the dynamics of crowds in panic or evacuation situations, methods to optimize building designs for egress, and factors potentially causing the breakdown of orderly motion.

2 Glossary

Collective Intelligence: Emergent functional behavior of a large number of people that results from *interactions* of individuals rather than from individual reasoning or global optimization.

Crowd: Agglomeration of many people in the same area at the same time. The density of the crowd is assumed to be high enough to cause continuous interactions with or reactions to other individuals.

Crowd Turbulence: Unanticipated and unintended irregular motion of individuals into different directions due to strong and rapidly changing forces in crowds of extreme density.

Emergence: Spontaneous establishment of a qualitatively new behavior through non-linear interactions of many objects or subjects.

Evolutionary Optimization: Gradual optimization based on the effect of frequently repeated random mutations and selection processes based on some success function (“fitness”).

Faster-is-Slower Effect: This term reflects the observation that certain processes (in evacuation situations, production, traffic dynamics, or logistics) take more time if performed at high speed. In other words, waiting can often help to coordinate the activities of several competing units and to speed up the average progress.

Freezing-by-Heating Effect: Noise-induced blockage effect caused by the breakdown of direction-segregated walking patterns (typically two or more “lanes” characterized by a uniform direction of motion). “Noise” means frequent variations of the walking direction due to nervousness or impatience in the crowd, e.g. also frequent overtaking maneuvers in dense, slowly moving crowds.

Panic: Breakdown of ordered, cooperative behavior of individuals due to anxious reactions to a certain event. Often, panic is characterized by attempted escape of many individuals from a real or perceived threat in situations of imminent danger, which may end up in trampling or crushing of people in a crowd. Definitions of the term “panic” are controversial and depend on the discipline or community of people using it.

Self-Organization: Spontaneous organization (i.e. formation of ordered patterns) not induced by initial or boundary conditions, by regulations or constraints. Self-organization is a result of non-linear interactions between many objects or subjects, and it often causes different kinds of spatio-temporal patterns of motion.

Social Force: Vector describing acceleration or deceleration effects that are caused by social interactions rather than by physical interactions or fields.

3 Definition

The modeling of pedestrian motion is of great theoretical and practical interest. Recent experimental efforts have revealed quantitative details of pedestrian interactions, which have been successfully cast into mathematical equations. Furthermore, corresponding computer simulations of large numbers of pedestrians have been compared with the empirically observed dynamics of crowds. Such studies have led to a deeper understanding of how collective behavior on a macroscopic scale emerges from individual human interactions. Interestingly enough, the non-linear interactions of pedestrians lead to various complex, spatio-temporal pattern-formation phenomena. This includes the emergence of lanes of uniform walking direction, oscillations of the pedestrian flow at bottlenecks, and the formation of stripes in two intersecting flows. Such self-organized patterns of motion demonstrate that an efficient, “intelligent” collective dynamics can be based on simple, local interactions. Under extreme conditions, however, coordination may break down, giving rise to critical crowd conditions. Examples are “freezing-by-heating” and “faster-is-slower” effects, but also the transition to “turbulent” crowd dynamics. These observations have important implications for the optimization of pedestrian facilities, in particular for evacuation situations.

4 Introduction

The emergence of new, functional or complex collective behaviors in social systems has fascinated many scientists. One of the primary questions in this field is how cooperation or coordination patterns originate based on elementary individual interactions. While one could think that these are a result of intelligent human actions, it turns out that much simpler models assuming automatic responses can reproduce the observations very well. This suggests that humans are using their intelligence primarily for more complicated tasks, but also that simple interactions can lead to intelligent patterns of motion. Of course, it is reasonable to assume that these interactions are the result of a previous learning process

that has optimized the automatic response in terms of minimizing collisions and delays. This, however, seems to be sufficient to explain most observations.

Note, however, that research into pedestrian and crowd behavior is highly multi-disciplinary. It involves activities of traffic scientists, psychologists, sociologists, biologists, physicists, computer scientists, and others. Therefore, it is not surprising that there are sometimes different or even controversial views on the subject, e.g. with regard to the concept of “panic”, the explanation of collective, spatio-temporal patterns of motion in pedestrian crowds, the best modeling concept, or the optimal number of parameters of a model.

In this contribution, we will start with a short history of pedestrian modeling and, then, introduce the wide-spread “social force model” of pedestrian interactions to illustrate further issues such as, for example, model calibration by video tracking data. Next, we will turn to the subject of crowd dynamics, since one typically finds the formation of large-scale spatio-temporal patterns of motion, when many pedestrians interact with each other. These patterns will be discussed in some detail before we will turn to evacuation situations and cases of extreme densities, where one can sometimes observe the breakdown of coordination. Finally, we will address possibilities to design improved pedestrian facilities, using special evolutionary algorithms.

5 Pedestrian Dynamics

5.1 Short History of Pedestrian Modeling

Pedestrians have been empirically studied for more than four decades [1,2,3]. The evaluation methods initially applied were based on direct observation, photographs, and time-lapse films. For a long time, the main goal of these studies was to develop a *level-of-service concept* [4], *design elements* of pedestrian facilities [5,6,7,8], or *planning guidelines* [9,10]. The latter have usually the form of *regression relations*, which are, however, not very well suited for the prediction of pedestrian flows in pedestrian zones and buildings with an exceptional architecture, or in challenging evacuation situations. Therefore, a number of simulation models have been proposed, e.g. *queueing models* [11], *transition matrix models* [12], and *stochastic models* [13], which are partly related to each other. In addition, there are models for the *route choice behavior* of pedestrians [14,15].

None of these concepts adequately takes into account the self-organization effects occurring in pedestrian crowds. These are the subject of recent experimental studies [8,16,17,18,19,20]. Most pedestrian models, however, were formulated before. A first modeling approach that appears to be suited to reproduce spatio-temporal patterns of motion was proposed by Henderson [21], who conjectured that pedestrian crowds behave similar to gases or fluids (see also [22]). This could be partially confirmed, but a realistic gas-kinetic or fluid-dynamic theory for pedestrians must contain corrections due to their particular interactions (i.e. avoidance and deceleration maneuvers) which, of course, do not obey momentum and energy conservation. Although such a theory can be actually

formulated [23,24], for practical applications a direct simulation of *individual* pedestrian motion is favourable, since this is more flexible. As a consequence, pedestrian research mainly focusses on *agent-based models* of pedestrian crowds, which also allow one to consider local coordination problems. The “social force model” [25,26] is maybe the most well-known of these models, but we also like to mention *cellular automata* of pedestrian dynamics [27,28,29,30,31,32,33] and *AI-based models* [34,35].

5.2 The Social Force Concept

In the following, we shall shortly introduce the social force concept, which reproduces most empirical observations in a simple and natural way. Human behavior often seems to be “chaotic”, irregular, and unpredictable. So, why and under what conditions can we model it by means of forces? First of all, we need to be confronted with a phenomenon of motion in some (quasi-)continuous space, which may be also an abstract behavioral space such as an opinion scale [36]. Moreover, it is favourable to have a system where the fluctuations due to unknown influences are not large compared to the systematic, deterministic part of motion. This is usually the case in pedestrian traffic, where people are confronted with standard situations and react “automatically” rather than taking complicated decisions, e.g. if they have to evade others.

This “automatic” behavior can be interpreted as the result of a *learning process* based on trial and error [37], which can be simulated with *evolutionary algorithms* [38]. For example, pedestrians have a preferred side of walking, since an asymmetrical avoidance behavior turns out to be profitable [25,37]. The related *formation of a behavioral convention* can be described by means of *evolutionary game theory* [25,39].

Another requirement is the vectorial additivity of the separate force terms reflecting different environmental influences. This is probably an approximation, but there is some experimental evidence for it. Based on quantitative measurements for animals and test persons subject to separately or simultaneously applied stimuli of different nature and strength, one could show that the behavior in conflict situations can be described by a superposition of forces [40,41]. This fits well into a concept by Lewin [42], according to which behavioral changes are guided by so-called *social fields* or *social forces*, which has later on been put into mathematical terms [25,43]. In some cases, social forces, which determine the amount and direction of systematic behavioral changes, can be expressed as gradients of dynamically varying potentials, which reflect the social or behavioral fields resulting from the interactions of individuals. Such a social force concept was applied to opinion formation and migration [43], and it was particularly successful in the description of collective pedestrian behavior [8,25,26,37].

For reliable simulations of pedestrian crowds, we do not need to know whether a certain pedestrian, say, turns to the right at the next intersection. It is sufficient to have a good estimate what percentage of pedestrians turns to the right. This can be either empirically measured or estimated by means of route choice models [14]. In some sense, the uncertainty about the individual behaviors is

averaged out at the macroscopic level of description. Nevertheless, we will use the more flexible microscopic simulation approach based on the social force concept. According to this, the temporal change of the location $\mathbf{r}_\alpha(t)$ of pedestrian α obeys the equation

$$\frac{d\mathbf{r}_\alpha(t)}{dt} = \mathbf{v}_\alpha(t). \quad (1)$$

Moreover, if $\mathbf{f}_\alpha(t)$ denotes the sum of social forces influencing pedestrian α and if $\boldsymbol{\xi}_\alpha(t)$ are individual fluctuations reflecting unsystematic behavioral variations, the velocity changes are given by the *acceleration equation*

$$\frac{d\mathbf{v}_\alpha}{dt} = \mathbf{f}_\alpha(t) + \boldsymbol{\xi}_\alpha(t). \quad (2)$$

A particular advantage of this approach is that we can take into account the flexible usage of space by pedestrians, requiring a continuous treatment of motion. It turns out that this point is essential to reproduce the empirical observations in a natural and robust way, i.e. without having to adjust the model to each single situation and measurement site. Furthermore, it is interesting to note that, if the fluctuation term is neglected, the social force model can be interpreted as a particular *differential game*, i.e. its dynamics can be derived from the minimization of a special utility function [44].

5.3 Specification of the Social Force Model

The social force model for pedestrians assumes that each individual α is trying to move in a desired direction \mathbf{e}_α^0 with a desired speed v_α^0 , and that it adapts the actual velocity \mathbf{v}_α to the desired one, $\mathbf{v}_\alpha^0 = v_\alpha^0 \mathbf{e}_\alpha^0$, within a certain relaxation time τ_α . The systematic part $\mathbf{f}_\alpha(t)$ of the acceleration force of pedestrian α is then given by

$$\mathbf{f}_\alpha(t) = \frac{1}{\tau_\alpha} (v_\alpha^0 \mathbf{e}_\alpha^0 - \mathbf{v}_\alpha) + \sum_{\beta(\neq\alpha)} \mathbf{f}_{\alpha\beta}(t) + \sum_i \mathbf{f}_{\alpha i}(t), \quad (3)$$

where the terms $\mathbf{f}_{\alpha\beta}(t)$ and $\mathbf{f}_{\alpha i}(t)$ denote the repulsive forces describing attempts to keep a certain safety distance to other pedestrians β and obstacles i . In very crowded situations, additional physical contact forces come into play (see Sec. 7.3). Further forces may be added to reflect attraction effects between members of a group or other influences. For details see Ref. [37].

First, we will assume a simplified interaction force of the form

$$\mathbf{f}_{\alpha\beta}(t) = \mathbf{f}(\mathbf{d}_{\alpha\beta}(t)), \quad (4)$$

where $\mathbf{d}_{\alpha\beta} = \mathbf{r}_\alpha - \mathbf{r}_\beta$ is the distance vector pointing from pedestrian β to α . Angular-dependent shielding effects may be furthermore taken into account by a prefactor describing the anisotropic reaction to situations in front of as

compared to behind a pedestrian [26,45], see Sec. 5.4. However, we will start with a **circular specification** of the distance-dependent interaction force,

$$\mathbf{f}(\mathbf{d}_{\alpha\beta}) = A_\alpha e^{-d_{\alpha\beta}/B_\alpha} \frac{\mathbf{d}_{\alpha\beta}}{\|\mathbf{d}_{\alpha\beta}\|}, \quad (5)$$

where $d_{\alpha\beta} = \|\mathbf{d}_{\alpha\beta}\|$ is the distance. The parameter A_α reflects the *interaction strength*, and B_α corresponds to the *interaction range*. While the dependence on α explicitly allows for a dependence of these parameters on the single individual, we will assume a homogeneous population, i.e. $A_\alpha = A$ and $B_\alpha = B$ in the following. Otherwise, it would be hard to collect enough data for parameter calibration.

Elliptical specification: Note that it is possible to express Eq. (5) as gradient of an exponentially decaying potential $V_{\alpha\beta}$. This circumstance can be used to formulate a generalized, elliptical interaction force via the potential

$$V_{\alpha\beta}(b_{\alpha\beta}) = AB e^{-b_{\alpha\beta}/B}, \quad (6)$$

where the variable $b_{\alpha\beta}$ denotes the semi-minor axis $b_{\alpha\beta}$ of the elliptical equipotential lines. This has been specified according to

$$2b_{\alpha\beta} = \sqrt{(\|\mathbf{d}_{\alpha\beta}\| + \|\mathbf{d}_{\alpha\beta} - (\mathbf{v}_\beta - \mathbf{v}_\alpha)\Delta t\|)^2 - \|(\mathbf{v}_\beta - \mathbf{v}_\alpha)\Delta t\|^2}, \quad (7)$$

so that both pedestrians α and β are treated symmetrically. The repulsive force is related to the above potential via

$$\mathbf{f}_{\alpha\beta}(\mathbf{d}_{\alpha\beta}) = -\nabla_{\mathbf{d}_{\alpha\beta}} V_{\alpha\beta}(b_{\alpha\beta}) = -\frac{dV_{\alpha\beta}(b_{\alpha\beta})}{db_{\alpha\beta}} \nabla_{\mathbf{d}_{\alpha\beta}} b_{\alpha\beta}(\mathbf{d}_{\alpha\beta}), \quad (8)$$

where $\nabla_{\mathbf{d}_{\alpha\beta}}$ represents the gradient with respect to $\mathbf{d}_{\alpha\beta}$. Considering the chain rule, $\|\mathbf{z}\| = \sqrt{\mathbf{z}^2}$, and $\nabla_{\mathbf{z}}\|\mathbf{z}\| = \mathbf{z}/\sqrt{\mathbf{z}^2} = \mathbf{z}/\|\mathbf{z}\|$, this leads to the explicit formula

$$\mathbf{f}_{\alpha\beta}(\mathbf{d}_{\alpha\beta}) = Ae^{-b_{\alpha\beta}/B} \cdot \frac{\|\mathbf{d}_{\alpha\beta}\| + \|\mathbf{d}_{\alpha\beta} - \mathbf{y}_{\alpha\beta}\|}{2b_{\alpha\beta}} \cdot \frac{1}{2} \left(\frac{\mathbf{d}_{\alpha\beta}}{\|\mathbf{d}_{\alpha\beta}\|} + \frac{\mathbf{d}_{\alpha\beta} - \mathbf{y}_{\alpha\beta}}{\|\mathbf{d}_{\alpha\beta} - \mathbf{y}_{\alpha\beta}\|} \right) \quad (9)$$

with $\mathbf{y}_{\alpha\beta} = (\mathbf{v}_\beta - \mathbf{v}_\alpha)\Delta t$. We used $\Delta t = 0.5\text{s}$. For $\Delta t = 0$, we regain the expression of Eq. (5).

The elliptical specification has two major advantages compared to the circular one: First, the interactions depend not only on the distance, but also on the relative velocity. Second, the repulsive force is not strictly directed from pedestrian β to pedestrian α , but has a lateral component. As a consequence, this leads to less confrontative, smoother (“sliding”) evading maneuvers. Note that further velocity-dependent specifications of pedestrian interaction forces have been proposed [7,26], but we will restrict to the above specifications, as these are sufficient to demonstrate the method of evolutionary model calibration. For suggested improvements regarding the specification of social forces see, for example, Refs. [46,47].

5.4 Angular Dependence

In reality, of course, pedestrian interactions are not isotropic, but dependent on the angle $\varphi_{\alpha\beta}$ of the encounter, which is given by the formula

$$\cos(\varphi_{\alpha\beta}) = \frac{\mathbf{v}_\alpha}{\|\mathbf{v}_\alpha\|} \cdot \frac{-\mathbf{d}_{\alpha\beta}}{\|\mathbf{d}_{\alpha\beta}\|}. \quad (10)$$

Generally, pedestrians show little response to pedestrians behind them. This can be reflected by an angular-dependent prefactor $w(\varphi_{\alpha\beta})$ of the interaction force [45]. Empirical results are represented in Fig. 2 (right). Reasonable results are obtained for the following specification of the prefactor:

$$w(\varphi_{\alpha\beta}(t)) = \left(\lambda_\alpha + (1 - \lambda_\alpha) \frac{1 + \cos(\varphi_{\alpha\beta})}{2} \right), \quad (11)$$

where λ_α with $0 \leq \lambda_\alpha \leq 1$ is a parameter which grows with the strength of interactions from behind. An evolutionary parameter optimization gives values $\lambda \approx 0.1$ (see Sec. 5.5, i.e. a strong anisotropy. Other angular-dependent specifications split up the interaction force between pedestrians into a component against the direction of motion and another one perpendicular to it. Such a description allows for even smoother avoidance maneuvers.

5.5 Evolutionary Calibration with Video Tracking Data

For parameter calibration, several video recordings of pedestrian crowds in different natural environments have been used. The dimensions of the recorded areas were known, and the floor tiling or environment provided something like a “coordinate system”. The heads were automatically determined by searching for round moving structures, and the accuracy of tracking was improved by comparing actual with linearly extrapolated positions (so it would not happen so easily that the algorithm interchanged or “lost” closeby pedestrians). The trajectories of the heads were then projected on two-dimensional space in a way correcting for distortion by the camera perspective. A representative plot of the resulting trajectories is shown in Fig. 1. Note that trajectory data have been obtained with infra-red sensors [48] or video cameras [49,50] for several years now, but algorithms that can simultaneously handle more than one thousand pedestrians have become available only recently [51].

For model calibration, it is recommended to use a hybrid method fusing empirical trajectory data and microscopic simulation data of pedestrian movement in space. In corresponding algorithms, a virtual pedestrian is assigned to each tracked pedestrian in the simulation domain. One then starts a simulation for a time period T (e.g. 1.5 seconds), in which one pedestrian α is moved according to a simulation of the social force model, while the others are moved exactly according to the trajectories extracted from the videos. This procedure is performed for all pedestrians α and for several different starting times t , using a fixed parameter set for the social force model.

Each simulation run is performed according to the following scheme:

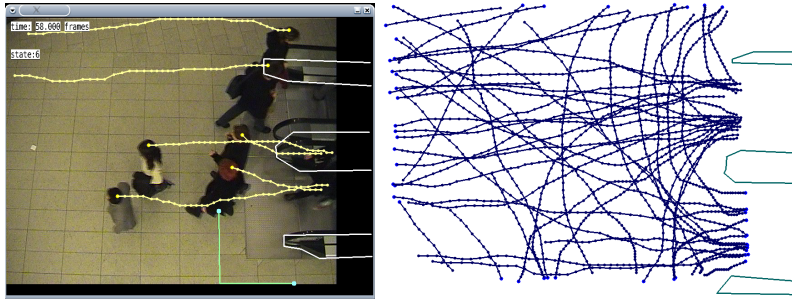


Fig. 1. Video tracking used to extract the trajectories of pedestrians from video recordings close to two escalators (after [45]). Left: Illustration of the tracking of pedestrian heads. Right: Resulting trajectories after being transformed onto the two-dimensional plane.

1. Define a starting point and calculate the state (position \mathbf{r}_α , velocity \mathbf{v}_α , and acceleration $\mathbf{a}_\alpha = d\mathbf{v}_\alpha/dt$) for each pedestrian α .
2. Assign a desired speed v_α^0 to each pedestrian, e.g. the maximum speed during the pedestrian tracking time. This is sufficiently accurate, if the overall pedestrian density is not too high and the desired speed is constant in time.
3. Assign a desired goal point for each pedestrian, e.g. the end point of the trajectory.
4. Given the tracked motion of the surrounding pedestrians β , simulate the trajectory of pedestrian α over a time period T based on the social force model, starting at the actual location $\mathbf{r}_\alpha(t)$.

After each simulation run, one determines the relative distance error

$$\frac{\|\mathbf{r}_\alpha^{\text{simulated}}(t+T) - \mathbf{r}_\alpha^{\text{tracked}}(t+T)\|}{\|\mathbf{r}_\alpha^{\text{tracked}}(t+T) - \mathbf{r}_\alpha^{\text{tracked}}(t)\|}. \quad (12)$$

After averaging the relative distance errors over the pedestrians α and starting times t , 1 minus the result can be taken as measure of the goodness of fit (the “fitness”) of the parameter set used in the pedestrian simulation. Hence, the best possible value of the “fitness” is 1, but any deviation from the real pedestrian trajectories implies lower values.

One result of such a parameter optimization is that, for each video, there is a broad range of parameter combinations of A and B which perform almost equally well [45]. This allows one to apply additional goal functions in the parameter optimization, e.g. to determine among the best performing parameter values such parameter combinations, which perform well for *several* video recordings, using a fitness function which equally weights the fitness reached in each single video. This is how the parameter values listed in Table 1 were determined. It turns out that, in order to reach a good model performance, the pedestrian interaction force must be specified velocity dependent, as in the elliptical model.

Model	A [m/s ²]	B [m]	λ	Fitness
Extrapolation	0	–	–	0.34
Circular	0.42 ± 0.26	1.65 ± 1.01	0.12 ± 0.07	0.40
Elliptical	0.04 ± 0.01	3.22 ± 0.67	0.06 ± 0.04	0.61

Table 1. Interaction strength A and interaction range B resulting from our evolutionary parameter calibration for the circular and elliptical specification of the interaction forces between pedestrians (see main text), with an assumed angular dependence according to Eq. (11). A comparison with the extrapolation scenario, which assumes constant speeds, allows one to judge the improvement in the goodness of fit (“fitness”) by the specified interaction force. The calibration was based on three different video recordings, one for low crowd density, one for medium, and one for high density (see Ref. [45] for details). The parameter values are specified as mean value \pm standard deviation. The best fitness value obtained with the elliptical specification for the video with the lowest crowd density was as high as 0.9.

Note that our evolutionary fitting method can be also used to determine interaction laws without prespecified interaction functions. For example, one can obtain the distance dependence of pedestrian interactions without a pre-specified function. For this, one adjusts the values of the force at given distances $d_k = kd_1$ (with $k \in \{1, 2, 3, \dots\}$) in an evolutionary way. To get some smoothness, linear interpolation is applied. The resulting fit curve is presented in Fig. 2 (left). It turns out that the empirical dependence of the force with distance can be well fitted by an exponential decay.

6 Crowd Dynamics

6.1 Analogies with gases, fluids, and granular media

When the density is low, pedestrians can move freely, and the observed crowd dynamics can be partially compared with the behavior of gases. At medium and high densities, however, the motion of pedestrian crowds shows some striking analogies with the motion of fluids:

1. Footprints of pedestrians in snow look similar to streamlines of fluids [15].
2. At borderlines between opposite directions of walking one can observe “viscous fingering” [52,53].
3. The emergence of pedestrian streams through standing crowds [7,37,54] appears analogous to the formation of river beds [55,56].

At high densities, however, the observations have rather analogies with driven granular flows. This will be elaborated in more detail in Secs. 7.3 and 7.4. In summary, one could say that fluid-dynamic analogies work reasonably well in normal situations, while granular aspects dominate at extreme densities. Nevertheless,

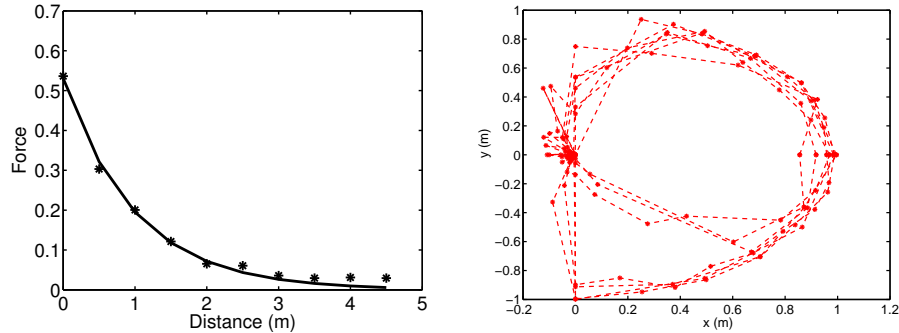


Fig. 2. Results of an evolutionary fitting of pedestrian interactions. Left: Empirically determined distance dependence of the interaction force between pedestrians. An exponential decay fits the empirical data quite well. The dashed fit curve corresponds to Eq. (5) with the parameters $A = 0.53$ and $B = 1.0$. Right: Angular dependence of the influence of other pedestrians. The direction along the positive x axis corresponds to the walking direction of pedestrians, y to the perpendicular direction. (After [45].)

the analogy is limited, since the self-driven motion and the violation of momentum conservation imply special properties of pedestrian flows. For example, one usually does not observe eddies.

6.2 Self-Organization of Pedestrian Crowds

Despite its simplifications, the social force model of pedestrian dynamics describes a lot of observed phenomena quite realistically. Especially, it allows one to explain various self-organized spatio-temporal patterns that are not externally planned, prescribed, or organized, e.g. by traffic signs, laws, or behavioral conventions [7,8,37]. Instead, the spatio-temporal patterns discussed below emerge due to the non-linear interactions of pedestrians even without assuming strategical considerations, communication, or imitative behavior of pedestrians. Despite this, we may still interpret the forming cooperation patterns as phenomena that establish social order on short time scales. It is actually surprising that strangers coordinate each other within seconds, if they have grown up in a similar environment. People from different countries, however, are sometimes irritated about local walking habits, which indicates that learning effects and cultural backgrounds still play a role in social interactions as simple as random pedestrian encounters. Rather than on particular features, however, in the following we will focus on the common, internationally reproducible observations.

Lane formation: In pedestrian flows one can often observe that oppositely moving pedestrians are forming lanes of uniform walking direction (see Fig. 3) [8,20,25,26]. This phenomenon even occurs when there is not a large distance to

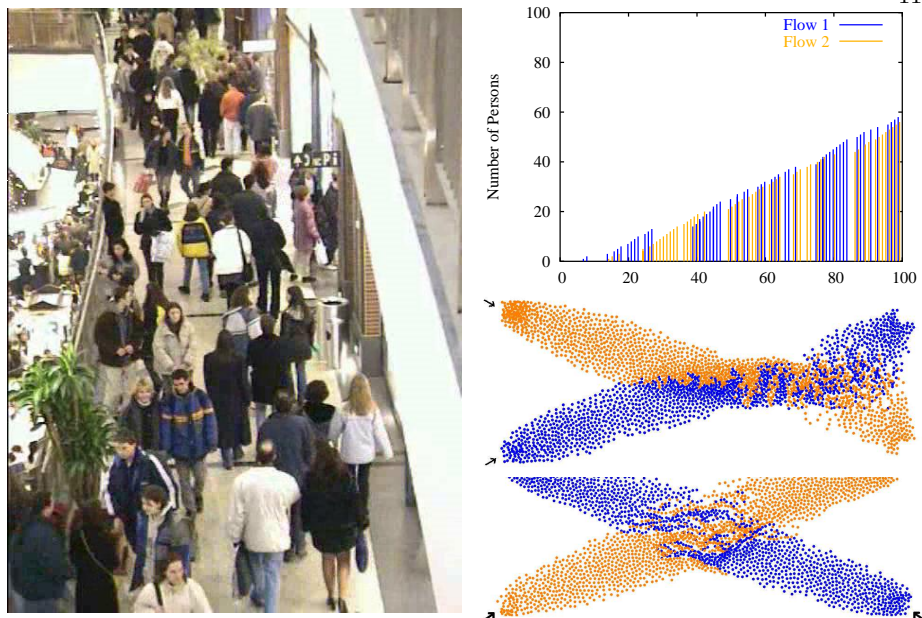


Fig. 3. Self-organization of pedestrian crowds. Left: Photograph of lanes formed in a shopping center. Computer simulations reproduce the self-organization of such lanes very well. Top right: Evaluation of the cumulative number of pedestrians passing a bottleneck from different sides. One can clearly see that the narrowing is often passed by groups of people in an oscillatory way rather than one by one. Bottom right: Multi-agent simulation of two crossing pedestrian streams, showing the phenomenon of stripe formation. This self-organized pattern allows pedestrians to pass the other stream without having to stop, namely by moving sideways in a forwardly moving stripe. (After Ref. [8].)

separate each other, e.g. on zebra crossings. However, the width of lanes increases (and their number decreases), if the interaction continues over longer distances (and if perturbations, e.g. by flows entering or leaving on the sides, are low; otherwise the phenomenon of lane formation may break down [57]).

Lane formation may be viewed as *segregation phenomenon* [58,59]. Although there is a weak preference for one side (with the corresponding behavioral convention depending on the country), the observations can only be well reproduced when repulsive pedestrian interactions are taken into account. The most relevant factor for the lane formation phenomenon is the higher relative velocity of pedestrians walking in opposite directions. Compared to people following each other, oppositely moving pedestrians have more frequent interactions until they have segregated into separate lanes by stepping aside whenever another pedestrian is encountered. The most long-lived patterns of motion are the ones which change the least. It is obvious that such patterns correspond to lanes, as they minimize the frequency and strength of avoidance maneuvers. Interestingly enough, as

computer simulations show, lane formation occurs also when there is no preference for any side.

Lanes minimize frictional effects, accelerations, energy consumption, and delays in oppositely moving crowds. Therefore, one could say that they are a pattern reflecting “collective intelligence”. In fact, it is not possible for a single pedestrian to reach such a collective pattern of motion. Lane formation is a self-organized collaborative pattern of motion originating from simple pedestrian interactions. Particularly in cases of no side preference, the system behavior cannot be understood by adding up the behavior of the single individuals. This is a typical feature of complex, self-organizing systems and, in fact, a wide-spread characteristics of social systems. It is worth noting, however, that it does not require a conscious behavior to reach forms of social organization like the segregation of oppositely moving pedestrians into lanes. This organization occurs automatically, although most people are not even aware of the existence of this phenomenon.

Oscillatory flows at bottlenecks: At bottlenecks, bidirectional flows of moderate density are often characterized by oscillatory changes in the flow direction (see Fig. 3) [8,26]. For example, one can sometimes observe this at entrances of museums during crowded art exhibitions or at entrances of staff canteens during lunch time. While these oscillatory flows may be interpreted as an effect of friendly behavior (“you go first, please”), computer simulations of the social force model indicate that the collective behavior may again be understood by simple pedestrian interactions. That is, oscillatory flows can even occur in the absence of communication, although it may be involved in reality. The interaction-based mechanism of oscillatory flows suggests to interpret them as another self-organization phenomenon, which again reduces frictional effects and delays. That is, oscillatory flows have features of “collective intelligence”.

While this may be interpreted as result of a learning effect in a large number of similar situations (a “repeated game”), our simulations suggest an even simpler, “many-particle” interpretation: Once a pedestrian is able to pass the narrowing, pedestrians with the same walking direction can easily follow. Hence, the number and “pressure” of waiting, “pushy” pedestrians on one side of the bottleneck becomes less than on the other side. This eventually increases their chance to occupy the passage. Finally, the “pressure difference” is large enough to stop the flow and turn the passing direction at the bottleneck. This reverses the situation, and eventually the flow direction changes again, giving rise to oscillatory flows.

At bottlenecks, further interesting observations can be made: Hoogendoorn and Daamen [60] report the formation of layers in unidirectional bottleneck flows. Due to the partial overlap of neighboring layers, there is a zipper effect. Moreover, Kretz *et al.* [61] have observed that the specific flow through a narrow bottleneck decreases with a growing width of the bottleneck, as long as it can be passed by one person at a time only. This is due to mutual obstructions, if two people are trying to enter the bottleneck simultaneously. If the opening is

large enough to be entered by several people in parallel, the specific flow stays constant with increasing width. Space is then used in a flexible way.

Stripe formation in intersecting flows: In intersection areas, the flow of people often appears to be irregular or “chaotic”. In fact, it can be shown that there are several possible collective patterns of motion, among them rotary and oscillating flows. However, these patterns continuously compete with each other, and a temporarily dominating pattern is destroyed by another one after a short time. Obviously, there has not evolved any social convention that would establish and stabilize an ordered and efficient flow at intersections.

Self-organized patterns of motion, however, are found in situations where pedestrian flows cross each other only in two directions. In such situations, the phenomenon of stripe formation is observed [62]. Stripe formation allows two flows to penetrate each other without requiring the pedestrians to stop. For an illustration see Fig. 3. Like lanes, stripes are a segregation phenomenon, but not a stationary one. Instead, the stripes are density waves moving into the direction of the sum of the directional vectors of both intersecting flows. Naturally, the stripes extend sideways into the direction which is perpendicular to their direction of motion. Therefore, the pedestrians move forward *with* the stripes and sideways *within* the stripes. Lane formation corresponds to the particular case of stripe formation where both directions are exactly opposite. In this case, no intersection takes place, and the stripes do not move systematically. As in lane formation, stripe formation allows to minimize obstructing interactions and to maximize the average pedestrian speeds, i.e. simple, repulsive pedestrian interactions again lead to an “intelligent” collective behavior.

7 Evacuation Dynamics

While the previous section has focussed on the dynamics of pedestrian crowds in normal situations, we will now turn to the description of situations in which extreme crowd densities occur. Such situations may arise at mass events, particularly in cases of urgent egress. While most evacuations run relatively smoothly and orderly, the situation may also get out of control and end up in terrible crowd disasters (see Tab. 2). In such situations, one often speaks of “panic”, although, from a scientific standpoint, the use of this term is rather controversial. Here, however, we will not be interested in the question whether “panic” actually occurs or not. We will rather focus on the issue of crowd dynamics at high densities and under psychological stress.

7.1 Evacuation and Panic Research

Computer models have been also developed for emergency and evacuation situations [32,63,64,65,66,67,68,69,70,71]. Most research into panic, however, has been of empirical nature (see, e.g. Refs. [72,73,74]), carried out by social psychologists and others.

With some exceptions, panic is thought to occur in cases of scarce or dwindling resources [75,76], which are either required for survival or anxiously desired. They are usually distinguished into escape panic (“stampedes”, bank or stock market panic) and acquisitive panic (“crazes”, speculative manias) [77,78], but in some cases this classification is questionable [79].

It is often stated that panicking people are obsessed by short-term personal interests uncontrolled by social and cultural constraints [76,77]. This is possibly a result of the reduced attention in situations of fear [76], which also causes that options like side exits are mostly ignored [72]. It is, however, mostly attributed to social contagion [73,75,76,77,78,79,80,81,82,83,84], i.e., a transition from individual to mass psychology, in which individuals transfer control over their actions to others [78], leading to conformity [85]. This “herding behavior” is in some sense irrational, as it often leads to bad overall results like dangerous overcrowding and slower escape [72,78,79]. In this way, herding behavior can increase the fatalities or, more generally, the damage in the crisis faced.

The various socio-psychological theories for this contagion assume hypnotic effects, rapport, mutual excitation of a primordial instinct, circular reactions, social facilitation (see the summary by Brown [83]), or the emergence of normative support for selfish behavior [84]. Brown [83] and Coleman [78] add another explanation related to the prisoner’s dilemma [86,87] or common goods dilemma [88], showing that it is reasonable to make one’s subsequent actions contingent upon those of others. However, the socially favourable behavior of walking orderly is unstable, which normally gives rise to rushing by everyone. These thoughtful considerations are well compatible with many aspects discussed above and with the classical experiments by Mintz [75], which showed that jamming in escape situations depends on the reward structure (“payoff matrix”).

Nevertheless and despite of the frequent reports in the media and many published investigations of crowd disasters (see Table 2), a quantitative understanding of the observed phenomena in panic stampedes was lacking for a long time. The following sections will close this gap.

7.2 Situations of “Panic”

Panic stampede is one of the most tragic collective behaviors [73,74,75,77,78,80,81,82,83,84], as it often leads to the death of people who are either crushed or trampled down by others. While this behavior may be comprehensible in life-threatening situations like fires in crowded buildings [72,76], it is hard to understand in cases of a rush for good seats at a pop concert [79] or without any obvious reasons. Unfortunately, the frequency of such disasters is increasing (see Table 2), as growing population densities combined with easier transportation lead to greater mass events like pop concerts, sport events, and demonstrations. Nevertheless, systematic empirical studies of panic [75,90] are rare [76,77,79], and there is a scarcity of quantitative theories capable of predicting crowd dynamics at extreme densities [32,63,64,67,68,71]. The following features appear to be typical [57,91]:

1. In situations of escape panic, individuals are getting nervous, i.e. they tend to develop blind actionism.

Table 2. Incomplete list of major crowd disasters since 1970 after J. F. Dickie in Ref. [89], <http://www.crowddynamics.com/Main/Crowddisasters.html>, http://SportsIllustrated.CNN.com/soccer/world/news/2000/07/09/stadium_disasters_ap/, and other internet sources, excluding fires, bomb attacks, and train or plane accidents. The number of injured people was usually a multiple of the fatalities.

Date	Place	Venue	Deaths	Reason
1971	Ibroy, UK	Stadium	66	Collapse of barriers
1974	Cairo, Egypt	Stadium	48	Crowds break barriers
1982	Moscow, USSR	Stadium	340	Re-entering fans after last minute goal
1988	Katmandu, Nepal	Stadium	93	Stampede due to hailstorm
1989	Hillsborough, Sheffield, UK	Stadium	96	Fans trying to force their way into the stadium
1990	New York City	Bronx	87	Illegal happy land social club
1990	Mena, Saudi Arabia	Pedestrian Tunnel	1426	Overcrowding
1994	Mena, Saudi Arabia	Jamarat Bridge	266	Overcrowding
1996	Guatemala City, Guatemala	Stadium	83	Fans trying to force their way into the stadium
1998	Mena, Saudi Arabia		118	Overcrowding
1999	Kerala, India	Hindu Shrine	51	Collapse of parts of the shrine
1999	Minsk, Belarus	Subway Station	53	Heavy rain at rock concert
2001	Ghana, West Africa	Stadium	> 100	Panic triggered by tear gas
2004	Mena, Saudi Arabia	Jamarat Bridge	251	Overcrowding
2005	Wai, India	Religious Procession	150	Overcrowding (and fire)
2005	Bagdad, Iraque	Religious Procession	> 640	Rumors regarding suicide bomber
2005	Chennai, India	Disaster Area	42	Rush for flood relief supplies
2006	Mena, Saudi Arabia	Jamarat Bridge	363	Overcrowding
2006	Pilippines	Stadium	79	Rush for game show tickets
2006	Ibb, Yemen	Stadium	51	Rally for Yemeni president

2. People try to move considerably faster than normal [9].
3. Individuals start pushing, and interactions among people become physical in nature.
4. Moving and, in particular, passing of a bottleneck frequently becomes incoordinated [75].
5. At exits, jams are building up [75]. Sometimes, intermittent flows or arching and clogging are observed [9].
6. The physical interactions in jammed crowds add up and can cause dangerous pressures up to 4,500 Newtons per meter [72,89], which can bend steel barriers or tear down brick walls.
7. The strength and direction of the forces acting in large crowds can suddenly change [51], pushing people around in an uncontrollable way. This may cause people to fall.
8. Escape is slowed down by fallen or injured people turning into “obstacles”.
9. People tend to show herding behavior, i.e., to do what other people do [76,81].
10. Alternative exits are often overlooked or not efficiently used in escape situations [72,76].

7.3 Force Model for Panicking Pedestrians

Additional, physical interaction forces $\mathbf{f}_{\alpha\beta}^{\text{ph}}$ come into play when pedestrians get so close to each other that they have physical contact (i.e. $d_{\alpha\beta} < r_{\alpha\beta} = r_\alpha + r_\beta$, where r_α means the “radius” of pedestrian α) [91]. In this case, which is mainly relevant to panic situations, we assume also a “body force” $k(r_{\alpha\beta} - d_{\alpha\beta})\mathbf{n}_{\alpha\beta}$ counteracting body compression and a “sliding friction force” $\kappa(r_{\alpha\beta} - d_{\alpha\beta})\Delta v_{\beta\alpha}^t \mathbf{t}_{\alpha\beta}$ impeding *relative* tangential motion. Inspired by the formulas for granular interactions [92,93], we assume

$$\mathbf{f}_{\alpha\beta}^{\text{ph}}(t) = k\Theta(r_{\alpha\beta} - d_{\alpha\beta})\mathbf{n}_{\alpha\beta} + \kappa\Theta(r_{\alpha\beta} - d_{\alpha\beta})\Delta v_{\beta\alpha}^t \mathbf{t}_{\alpha\beta}, \quad (13)$$

where the function $\Theta(z)$ is equal to its argument z , if $z \geq 0$, otherwise 0. Moreover, $\mathbf{t}_{\alpha\beta} = (-n_{\alpha\beta}^2, n_{\alpha\beta}^1)$ means the tangential direction and $\Delta v_{\beta\alpha}^t = (\mathbf{v}_\beta - \mathbf{v}_\alpha) \cdot \mathbf{t}_{\alpha\beta}$ the tangential velocity difference, while k and κ represent large constants. (Strictly speaking, friction effects already set in before pedestrians touch each other, because of the psychological tendency not to pass other individuals with a high relative velocity, when the distance is small.)

The interactions with the boundaries of walls and other obstacles are treated analogously to pedestrian interactions, i.e., if $d_{\alpha i}(t)$ means the distance to obstacle or boundary i , $\mathbf{n}_{\alpha i}(t)$ denotes the direction perpendicular to it, and $\mathbf{t}_{\alpha i}(t)$ the direction tangential to it, the corresponding interaction force with the boundary reads

$$\mathbf{f}_{\alpha i} = \{A_\alpha \exp[(r_\alpha - d_{\alpha i})/B_\alpha] + k\Theta(r_\alpha - d_{\alpha i})\}\mathbf{n}_{\alpha i} - \kappa\Theta(r_\alpha - d_{\alpha i})(\mathbf{v}_\alpha \cdot \mathbf{t}_{\alpha i})\mathbf{t}_{\alpha i}. \quad (14)$$

Finally, fire fronts are reflected by repulsive social forces similar those describing walls, but they are much stronger. The physical interactions, however, are qualitatively different, as people reached by the fire front become injured and immobile ($\mathbf{v}_\alpha = \mathbf{0}$).

7.4 Collective Phenomena in Situations of “Panic”

Inspired by the observations discussed in Sec. 7.2, we have simulated situations of “panic” escape in the computer, assuming the following features:

1. People are getting nervous, resulting in a higher level of fluctuations.
2. They are trying to escape from the source of panic, which can be reflected by a significantly higher desired velocity v_{α}^0 .
3. Individuals in complex situations, who do not know what is the right thing to do, orient at the actions of their neighbours, i.e. they tend to do what other people do. We will describe this by an additional herding interaction.

We will now discuss the fundamental collective effects which fluctuations, increased desired velocities, and herding behavior can have according to simulations. Note that, in contrast to other approaches, we do not assume or imply that individuals in panic or emergency situations would behave relentless and asocial, although they sometimes do.

Herding and ignorance of available exits: If people are not sure what is the best thing to do, there is a tendency to show a “herding behavior”, i.e. to imitate the behavior of others. Fashion, hypes and trends are examples for this. The phenomenon is also known from stock markets, and particularly pronounced when people are anxious. Such a situation is, for example, given if people need to escape from a smoky room. There, the evacuation dynamics is very different from normal leaving (see Fig. 4).

Under normal visibility, everybody easily finds an exit and uses more or less the shortest path. However, when the exit cannot be seen, evacuation is much less efficient and may take a long time. Most people tend to walk relatively straight into the direction in which they suspect an exit, but in most cases, they end up at a wall. Then, they usually move along it in one of the two possible directions, until they finally find an exit [18]. If they encounter others, there is a tendency to take a decision for one direction and move collectively. Also in case of acoustic signals, people may be attracted into the same direction. This can lead to over-crowded exits, while other exits are ignored. The same can happen even for normal visibility, when people are not well familiar with their environment and are not aware of the directions of the emergency exits.

Computer simulations suggest that neither individualistic nor herding behavior performs well [91]. Pure individualistic behavior means that each pedestrian finds an exit only accidentally, while pure herding behavior implies that the complete crowd is eventually moving into the same and probably congested direction, so that available emergency exits are not efficiently used. Optimal chances of survival are expected for a certain mixture of individualistic and herding behavior, where individualism allows *some* people to detect the exits and herding guarantees that successful solutions are imitated by small groups of others [91].

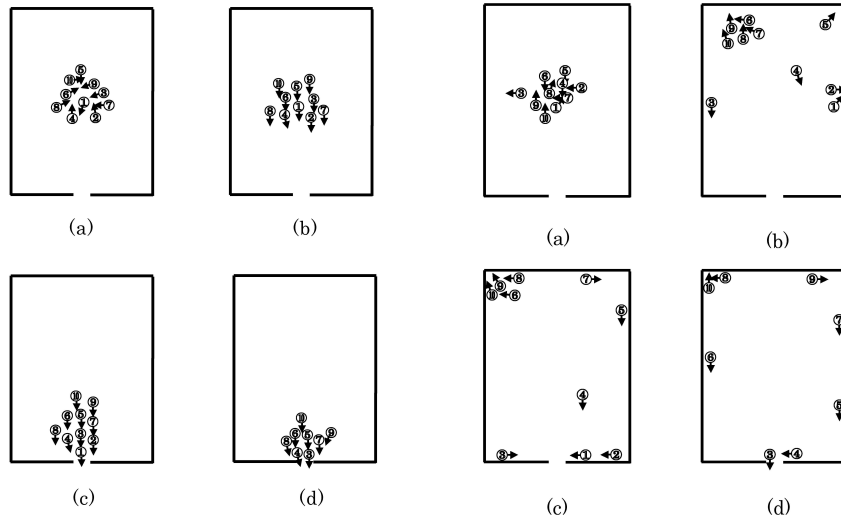


Fig. 4. Left: Normal leaving of a room, when the exit is well visible. Snapshots of a video-recorded experiment with 10 people after (a) $t = 0$ seconds (initial condition), (b) $t = 1$ sec., (c) $t = 3$ sec., and (d) $t = 5$ seconds. The face directions are indicated by arrows. Right: Escape from a room with no visibility, e.g. due to dense smoke or a power blackout. Snapshots of an experiment with test persons, whose eyes were covered by masks, after $t = 0$ seconds (initial condition), $t = 5$ sec., (c) $t = 10$ sec., and (d) $t = 15$ seconds. (After Ref. [18].)

“Freezing by heating”: Another effect of getting nervous has been investigated in Ref. [57]. Let us assume the individual fluctuation strength, i.e. the standard deviation of the noise term ξ_α , is given by

$$\eta_\alpha = (1 - n_\alpha)\eta_0 + n_\alpha\eta_{\max}, \quad (15)$$

where n_α with $0 \leq n_\alpha \leq 1$ measures the nervousness of pedestrian α . The parameter η_0 means the normal and η_{\max} the maximum fluctuation strength. It turns out that, at sufficiently high pedestrian densities, lanes are destroyed by increasing the fluctuation strength (which is analogous to the temperature). However, instead of the expected transition from the “fluid” lane state to a disordered, “gaseous” state, a “solid” state is formed. It is characterized by a blocked, “frozen” situation so that one calls this paradoxical transition “*freezing by heating*” (see Fig. 5). Notably enough, the blocked state has a *higher* degree of order, although the internal energy is *increased* [57].

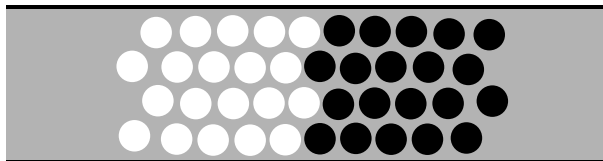


Fig. 5. Result of the noise-induced formation of a “frozen” state in a (periodic) corridor used by oppositely moving pedestrians (after Ref. [57]).

The preconditions for this unusual freezing-by-heating transition are the driving term $v_\alpha^0 e_\alpha^0 / \tau_\alpha$ and the dissipative friction $-v_\alpha / \tau_\alpha$, while the sliding friction force is not required. Inhomogeneities in the channel diameter or other impurities which temporarily slow down pedestrians can further this transition at the respective places. Finally note that a transition from fluid to blocked pedestrian counter flows is also observed, when a critical density is exceeded, as impatient pedestrians enter temporary gaps in the opposite lane to overtake others [31,57]. However, in contrast to computer simulations, resulting deadlocks are usually not permanent in real crowds, as turning the bodies (shoulders) often allows pedestrians to get out of the blocked area.

Intermittent flows, faster-is-slower effect, and “phantom panic”: If the overall flow towards a bottleneck is higher than the overall outflow from it, a pedestrian queue emerges [94]. In other words, a waiting crowd is formed upstream of the bottleneck. High densities can result, if people keep heading forward, as this eventually leads to higher and higher compressions. Particularly critical situations may occur if the arrival flow is much higher than the departure flow, especially if people are trying to get towards a strongly desired goal (“acquisitive panic”) or away from a perceived source of danger (“escape panic”) with

an increased driving force $v_\alpha^0 e_\alpha^0 / \tau$. In such situations, the high density causes coordination problems, as several people compete for the same few gaps. This typically causes body interactions and frictional effects, which can slow down crowd motion or evacuation (*“faster is slower effect”*).

A possible consequence of these coordination problems are intermittent flows. In such cases, the outflow from the bottleneck is not constant, but it is typically interrupted. While one possible origin of the intermittent flows are clogging and arching effects as known from granular flows through funnels or hoppers [92,93], stop-and-go waves have also been observed in more than 10 meter wide streets and in the 44 meters wide entrance area to the Jamarat Bridge during the pilgrimage in January 12, 2006 [51], see Fig. 6. Therefore, it seems to be important that people do not move continuously, but have minimum strides [25]. That is, once a person is stopped, he or she will not move until some space opens up in front. However, increasing impatience will eventually reduce the minimum stride, so that people eventually start moving again, even if the outflow through the bottleneck is stopped. This will lead to a further compression of the crowd.

In the worst case, such behavior can trigger a *“phantom panic”*, i.e. a crowd disaster *without* any serious reasons (e.g., in Moscow, 1982). For example, due to the *“faster-is-slower effect”* panic can be triggered by small pedestrian counterflows [72], which cause delays to the crowd intending to leave. Consequently, stopped pedestrians in the back, who do not see the reason for the temporary slowdown, are getting impatient and pushy. In accordance with observations [25,7], one may model this by increasing the desired velocity, for example, by the formula

$$v_\alpha^0(t) = [1 - n_\alpha(t)]v_\alpha^0(0) + n_\alpha(t)v_\alpha^{\max}. \quad (16)$$

Herein, v_α^{\max} is the maximum desired velocity and $v_\alpha^0(0)$ the initial one, corresponding to the expected velocity of leaving. The time-dependent parameter

$$n_\alpha(t) = 1 - \frac{\bar{v}_\alpha(t)}{v_\alpha^0(0)} \quad (17)$$

reflects the nervousness, where $\bar{v}_\alpha(t)$ denotes the average speed into the desired direction of motion. Altogether, long waiting times increase the desired speed v_α^0 or driving force $v_\alpha^0(t)e_\alpha^0/\tau$, which can produce high densities and inefficient motion. This further increases the waiting times, and so on, so that this tragic feedback can eventually trigger so high pressures that people are crushed or falling and trampled. It is, therefore, imperative, to have sufficiently wide exits and to prevent counterflows, when big crowds want to leave [91].

Transition to stop-and-go waves: Recent empirical studies of pilgrim flows in the area of Makkah, Saudi Arabia, have shown that intermittent flows occur not only when bottlenecks are obvious. On January 12, 2006, pronounced stop-and-go waves have been even observed upstream of the 44 meter wide entrance to the Jamarat Bridge [51]. While the pilgrim flows were smooth and continuous (*“laminar”*) over many hours, at 11:53am stop-and-go waves suddenly appeared

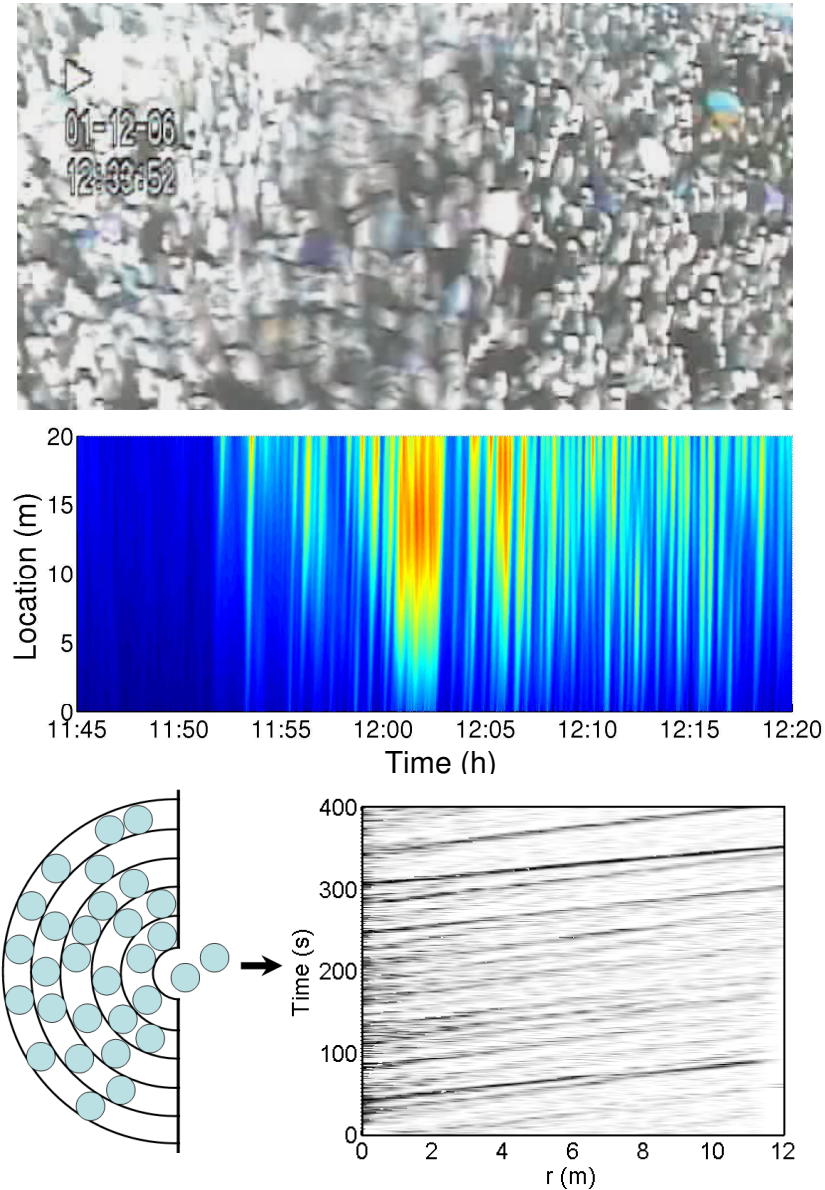


Fig. 6. Top: Long-term photograph showing stop-and-go waves in a densely packed street. While stopped people appear relatively sharp, people moving from right to left have a fuzzy appearance. Note that gaps propagate from left to right. Middle: Empirically observed stop-and-go waves in front of the entrance to the Jamarat Bridge on January 12, 2006 (after [51]), where pilgrims moved from left to right. Dark areas correspond to phases of motion, light colors to stop phases. The “location” coordinate represents the distance to the beginning of the narrowing, i.e. to the cross section of reduced width. Bottom left: Illustration of the “shell model” (see Ref. [94]), in particular of situations where several pedestrians compete for the same gap, which causes coordination problems. Bottom right: Simulation results of the shell model. The observed stop-and-go waves result from the alternation of forward pedestrian motion and backward gap propagation.

and propagated over distances of more than 30 meters (see Fig. 6). The sudden transition was related to a significant drop of the flow, i.e. with the onset of congestion [51]. Once the stop-and-go waves set in, they persisted over more than 20 minutes.

This phenomenon can be reproduced by a recent model based on two continuity equations, one for forward pedestrian motion and another one for backward gap propagation [94]. The model was derived from a “shell model” (see Fig. 6) and describes very well the observed alternation between backward gap propagation and forward pedestrian motion.

Transition to “crowd turbulence”: On the same day, around 12:19, the density reached even higher values and the video recordings showed a sudden transition from stop-and-go waves to *irregular* flows (see Fig. 7). These irregular flows were characterized by random, unintended displacements into all possible directions, which pushed people around. With a certain likelihood, this caused them to stumble. As the people behind were moved by the crowd as well and could not stop, fallen individuals were trampled, if they did not get back on their feet quickly enough. Tragically, the area of trampled people grew more and more in the course of time, as the fallen pilgrims became obstacles for others [51]. The result was one of the biggest crowd disasters in the history of pilgrimage.

How can we understand this transition to irregular crowd motion? A closer look at video recordings of the crowd reveals that, at this time, people were so densely packed that they were moved involuntarily by the crowd. This is reflected by random displacements into all possible directions. To distinguish these irregular flows from laminar and stop-and-go flows and due to their visual appearance, we will refer to them as “*crowd turbulence*”.

As in certain kinds of fluid flows, “turbulence” in crowds results from a sequence of instabilities in the flow pattern. Additionally, one finds a sharply peaked probability density function of velocity increments

$$V_x^\tau = V_x(\mathbf{r}, t + \tau) - V_x(\mathbf{r}, t), \quad (18)$$

which is typical for turbulence [95], if the time shift τ is small enough [51]. One also observes a power-law scaling of the displacements indicating self-similar behaviour [51]. As large eddies are not detected, however, the similarity with *fluid* turbulence is limited, but there is still an analogy to turbulence at currency exchange markets [95]. Instead of vortex cascades like in turbulent fluids, one rather finds a hierarchical fragmentation dynamics: At extreme densities, individual motion is replaced by mass motion, but there is a stick-slip instability which leads to “rupture” when the stress in the crowd becomes too large. That is, the mass splits up into clusters of different sizes with strong velocity correlations *inside* and distance-dependent correlations *between* the clusters.

“Crowd turbulence” has further specific features [51]. Due to the physical contacts among people in extremely dense crowds, we expect commonalities with granular media. In fact, dense driven granular media may form density waves, while moving forward [96], and can display turbulent-like states [97,98].

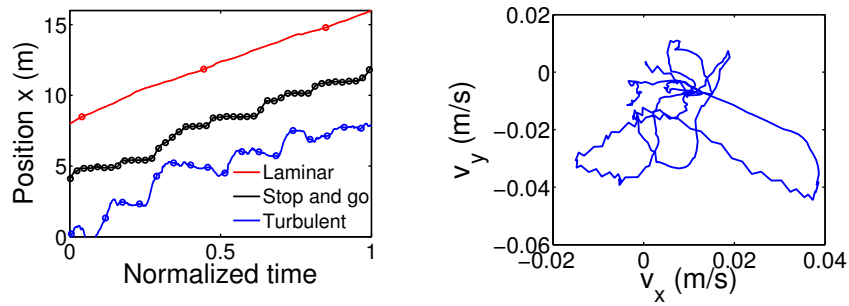


Fig. 7. Pedestrian dynamics at different densities. Left: Representative trajectories (space-time plots) of pedestrians during the laminar, stop-and-go, and turbulent flow regime. Each trajectory extends over a range of 8 meters, while the time required for this stretch is normalized to 1. To indicate the different speeds, symbols are included in the curves every 5 seconds. While the laminar flow (top line) is fast and smooth, motion is temporarily interrupted in stop-and-go flow (medium line), and backward motion can occur in “turbulent” flows (bottom line). Right: Example of the temporal evolution of the velocity components $v_x(t)$ into the average direction of motion and $v_y(t)$ perpendicular to it in “turbulent flow”, which occurs when the crowd density is extreme. One can clearly see the irregular motion into all possible directions characterizing “crowd turbulence”. For details see Ref. [51].

Moreover, under quasi-static conditions [97], force chains [99] are building up, causing strong variations in the strengths and directions of local forces. As in earthquakes [100,101] this can lead to events of sudden, uncontrollable stress release with power-law distributed displacements. Such a power-law has also been discovered by video-based crowd analysis [51].

7.5 Some Warning Signs of Critical Crowd Conditions

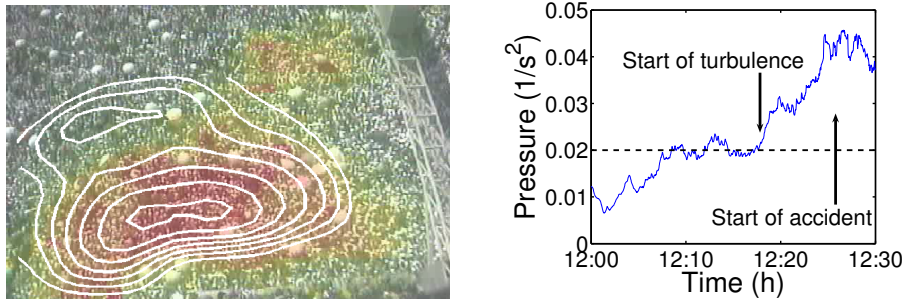


Fig. 8. Left: Snapshot of the on-line visualization of “crowd pressure”. Red colors (see the lower ellipses) indicate areas of critical crowd conditions. In fact, the sad crowd disaster during the Muslim pilgrimage on January 12, 2006, started in this area. Right: The “crowd pressure” is a quantitative measure of the onset of “crowd turbulence”. The crowd disaster started when the “crowd pressure” reached particularly high values. For details see Ref. [51].

Turbulent waves are experienced in dozens of crowd-intensive events each year all over the world [102]. Therefore, it is necessary to understand why, where and when potentially critical situations occur. Viewing real-time video recordings is not very suited to identify critical crowd conditions: While the average density rarely exceeds values of 6 persons per square meter, the local densities can reach almost twice as large values [51]. It has been found, however, that even evaluating the local densities is not enough to identify the critical times and locations precisely, which also applies to an analysis of the velocity field [51]. The decisive quantity is rather the “crowd pressure”, i.e. the density, multiplied with the variance of speeds. It allows one to identify critical locations and times (see Fig. 8).

There are even advance warning signs of critical crowd conditions: The crowd accident on January 12, 2006 started about 10 minutes after “turbulent” crowd motion set in, i.e. after the “pressure” exceeded a value of $0.02/s^2$ (see Fig. 8). Moreover, it occurred more than 30 minutes after stop-and-go waves set in, which can be easily detected in accelerated surveillance videos. Such advance warning

signs of critical crowd conditions can be evaluated on-line by an automated video analysis system. In many cases, this can help one to gain time for corrective measures like flow control, pressure-relief strategies, or the separation of crowds into blocks to stop the propagation of shockwaves [51]. Such anticipative crowd control could increase the level of safety during future mass events.

7.6 Evolutionary Optimization of Pedestrian Facilities

Having understood some of the main factors causing crowd disasters, it is interesting to ask how pedestrian facilities can be designed in a way that maximizes the efficiency of pedestrian flows and the level of safety. One of the major goals during mass events must be to avoid extreme densities. These often result from the onset of congestion at bottlenecks, which is a consequence of the breakdown of free flow and causes an increasing degree of compression. When a certain critical density is increased (which depends on the size distribution of people), this potentially implies high pressures in the crowd, particularly if people are impatient due to long delays or panic.

The danger of an onset of congestion can be minimized by avoiding bottlenecks. Notice, however, that jamming can also occur at widenings of escape routes [91]. This surprising fact results from disturbances due to pedestrians, who try to overtake each other and expand in the wider area because of their repulsive interactions. These squeeze into the main stream again at the end of the widening, which acts like a bottleneck and leads to jamming. The corresponding drop of efficiency E is more pronounced,

1. if the corridor is narrow,
2. if the pedestrians have different or high desired velocities, and
3. if the pedestrian density in the corridor is high.

Obviously, the emerging pedestrian flows decisively depend on the geometry of the boundaries. They can be simulated on a computer already in the planning phase of pedestrian facilities. Their configuration and shape can be systematically varied, e.g. by means of evolutionary algorithms [28,103] and evaluated on the basis of particular mathematical performance measures [7]. Apart from the *efficiency*

$$E = \frac{1}{N} \sum_{\alpha} \frac{\mathbf{v}_{\alpha} \cdot \mathbf{e}_{\alpha}^0}{v_{\alpha}^0} \quad (19)$$

we can, for example, define the *measure of comfort* $C = (1-D)$ via the discomfort

$$D = \frac{1}{N} \sum_{\alpha} \frac{\overline{(\mathbf{v}_{\alpha} - \bar{\mathbf{v}}_{\alpha})^2}}{(\bar{\mathbf{v}}_{\alpha})^2} = \frac{1}{N} \sum_{\alpha} \left(1 - \frac{\bar{\mathbf{v}}_{\alpha}^2}{(\bar{\mathbf{v}}_{\alpha})^2} \right). \quad (20)$$

The latter is again between 0 and 1 and reflects the frequency and degree of sudden velocity changes, i.e. the level of discontinuity of walking due to necessary avoidance maneuvers. Hence, the optimal configuration regarding the pedestrian requirements is the one with the highest values of efficiency and comfort.

During the optimization procedure, some or all of the following can be varied:

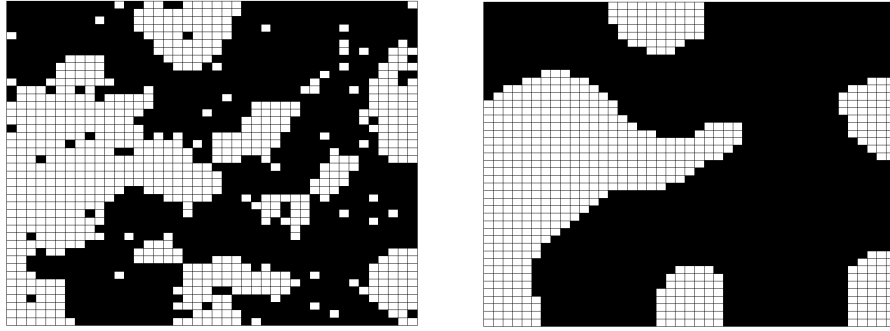


Fig. 9. The evolutionary optimization based on Boolean grids uses a two-stage algorithm (see Ref. [104] for details). Left: In the “randomization stage”, obstacles are distributed over the grid with some randomness, thereby allowing for the generation and testing of new topologies (architectures). Right: In the “agglomeration stage”, small nearby obstacles are clustered to form larger objects with smooth boundaries. After several iterations, the best performing designs are reasonably shaped. See Fig. 10 for examples of possible bottleneck designs.

1. the location and form of planned buildings,
2. the arrangement of walkways, entrances, exits, staircases, elevators, escalators, and corridors,
3. the shape of rooms, corridors, entrances, and exits,
4. the function and time schedule. (Recreation rooms or restaurants are often continuously frequented, rooms for conferences or special events are mainly visited and left at peak periods, exhibition rooms or rooms for festivities require additional space for people standing around, and some areas are claimed by queues or through traffic.)

In contrast to early evolutionary optimization methods, recent approaches allow to change not only the dimensions of the different elements of pedestrian facilities, but also to vary their topology. The procedure of such algorithms is illustrated in Fig. 9. Highly performing designs are illustrated in Fig. 10. It turns out that, for an emergency evacuation route, it is favorable if the crowd does not move completely straight towards a bottleneck. For example, a zigzag design of the evacuation route can reduce the pressure on the crowd upstream of a bottleneck (see Fig. 11). The proposed evolutionary optimization procedure can, of course, not only be applied to the design of new pedestrian facilities, but also to a reduction of existing bottlenecks, when suitable modifications are implemented.

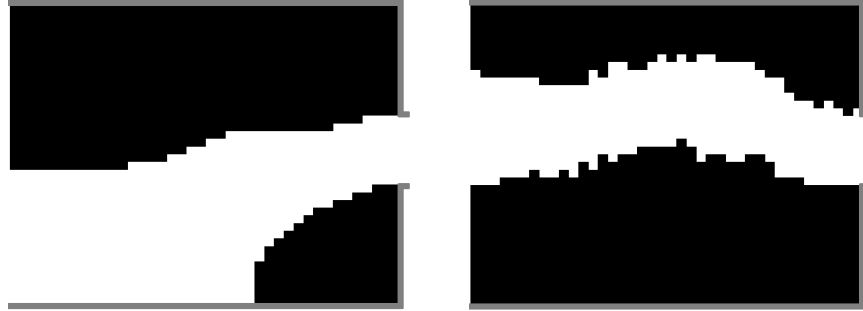


Fig. 10. Two examples of improved designs for cases with a bottleneck along the escape route of a large crowd, obtained with an evolutionary algorithm based on Boolean grids (after Ref. [104]). People were assumed to move from left to right only. Left: Funnel-shaped escape route. Right: Zig-zag design.

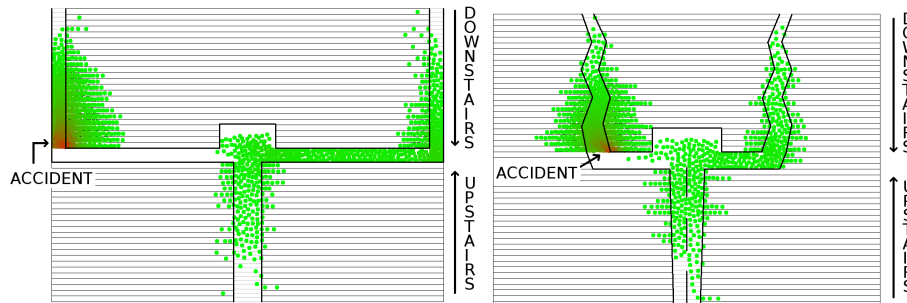


Fig. 11. Left: Conventional design of a stadium exit in an emergency scenario, where we assume that some pedestrians have fallen at the end of the downwards staircase to the left. The dark color indicates high pressures, since pedestrians are impatient and pushing from behind. Right: In the improved design, the increasing diameter of corridors can reduce waiting times and impatience (even with the same number of seats), thereby accelerating evacuation. Moreover, the zig-zag design of the downwards staircases changes the pushing direction in the crowd. Computer simulations indicate that the zig-zag design can reduce the average pressure in the crowd at the location of the incident by a factor of two. (After Ref. [8].)

8 Future Directions

In this contribution, we have presented a multi-agent approach to pedestrian and crowd dynamics. Despite the great effort required, pedestrian interactions can be well quantified by video tracking. Compared to other social interactions they turn out to be quite simple. Nevertheless, they cause a surprisingly large variety of self-organized patterns and short-lived social phenomena, where coordination or cooperation emerges spontaneously. For this reason, they are interesting to study, particularly as one can expect new insights into coordination mechanisms of social beings beyond the scope of classical game theory. Examples for observed self-organization phenomena in normal situations are lane formation, stripe formation, oscillations and intermittent clogging effects at bottlenecks, and the evolution of behavioral conventions (such as the preference of the right-hand side in continental Europe). Under extreme conditions (high densities or panic), however, coordination may break down, giving rise to “freezing-by-heating” or “faster-is-slower effects”, stop-and-go waves or “crowd turbulence”.

Similar observations as in pedestrian crowds are made in other social systems and settings. Therefore, we expect that realistic models of pedestrian dynamics will also promote the understanding of opinion formation and other kinds of collective behaviors. The hope is that, based on the discovered elementary mechanisms of emergence and self-organization, one can eventually also obtain a better understanding of the constituting principles of more complex social systems. At least the same underlying factors are found in many social systems: non-linear interactions of individuals, time-dependence, heterogeneity, stochasticity, competition for scarce resources (here: space and time), decision-making, and learning. Future work will certainly also address issues of perception, anticipation, and communication.

Acknowledgments

The authors are grateful for partial financial support by the German Research Foundation (research projects He 2789/7-1, 8-1) and by the “Cooperative Center for Communication Networks Data Analysis”, a NAP project sponsored by the Hungarian National Office of Research and Technology under grant No. KCKHA005.

References

Primary Literature

1. B. D. Hankin and R. A. Wright, *Operational Research Quarterly* 9, 81–88 (1958).
2. S. J. Older, *Traffic Engineering & Control* 10, 160–163 (1968).
3. U. Weidmann, *Transporttechnik der Fußgänger*, (Institut für Verkehrsplanung, Transporttechnik, Straßen- und Eisenbahnbau, ETH Zürich, 1993).
4. J. J. Fruin, *Designing for pedestrians: A level-of-service concept*, in *Highway Research Record, Number 355: Pedestrians*, pp. 1–15 (Highway Research Board, Washington, D.C., 1971).

5. J. Pauls, *Fire Technology* 20, 27–47 (1984).
6. W. H. Whyte, *City. Rediscovering the Center* (Doubleday, New York, 1988).
7. D. Helbing, *Verkehrsdynamik* (Springer, Berlin, 1997).
8. D. Helbing, L. Buzna, A. Johansson, and T. Werner, *Transportation Science* 39(1), 1-24 (2005).
9. W. M. Predtetschenski and A. I. Milinski, *Personenströme in Gebäuden – Berechnungsmethoden für die Projektierung –* (Rudolf Müller, Köln-Braunsfeld, 1971).
10. Transportation Research Board, *Highway Capacity Manual*, Special Report 209 (Transportation Research Board, Washington, D.C., 1985).
11. S. J. Yuhaski Jr., J. M. Macgregor Smith, *Queueing Systems* 4, 319–338 (1989).
12. D. Garbrecht, *Traffic Quarterly* 27, 89–109 (1973).
13. N. Ashford, M. O’Leary, and P. D. McGinity, *Traffic Engineering & Control* 17, 207–210 (1976).
14. A. Borgers and H. Timmermans, *Socio-Economic Planning Science* 20, 25–31 (1986).
15. D. Helbing, *Stochastische Methoden, nichtlineare Dynamik und quantitative Modelle sozialer Prozesse*, Ph.D. thesis (University of Stuttgart, 1992, published by Shaker, Aachen, 1993).
16. D. Helbing, M. Isobe, T. Nagatani, and K. Takimoto, *Physical Review E* 67, 067101 (2003).
17. W. Daamen and S. P. Hoogendoorn, in *Proceedings of the 82nd Annual Meeting at the Transportation Research Board* (CDROM, Washington D.C., 2003).
18. M. Isobe, D. Helbing, and T. Nagatani, *Physical Review E* 69, 066132 (2004).
19. A. Seyfried, B. Steffen, W. Klingsch, and M. Boltes, *J. Stat. Mech.* P10002 (2005).
20. T. Kretz, A. Grünebohm, M. Kaufman, F. Mazur, and M. Schreckenberg, *J. Stat. Mech.* P10001 (2006).
21. L. F. Henderson, *Transportation Research* 8, 509–515 (1974).
22. R. L. Hughes, *Transportation Research B* 36, 507–535 (2002).
23. D. Helbing, *Complex Systems* 6, 391–415 (1992).
24. S. P. Hoogendoorn and P. H. L. Bovy, *Transportation Research Records* 1710, 28–36 (2000).
25. D. Helbing, *Behavioral Science* 36, 298–310 (1991).
26. D. Helbing and P. Molnár, *Physical Review E* 51, 4282–4286 (1995).
27. P. G. Gipps and B. Marksjö, *Math. Comp. Simul.* 27, 95–105 (1985).
28. K. Bolay, *Nichtlineare Phänomene in einem fluid-dynamischen Verkehrsmodell* (Master’s thesis, University of Stuttgart, 1998).
29. V. J. Blue and J. L. Adler, *Transportation Research Records* 1644, 29–36 (1998).
30. M. Fukui and Y. Ishibashi, *Journal of the Physical Society of Japan* 68, 2861–2863 (1999).
31. M. Muramatsu, T. Irie, and T. Nagatani, *Physica A* 267, 487–498 (1999).
32. H. Klüpfel, M. Meyer-König, J. Wahle, and M. Schreckenberg, in S. Bandini and T. Worsch (eds.) *Theory and Practical Issues on Cellular Automata* (Springer, London, 2000).
33. C. Burstedde, K. Klauck, A. Schadschneider, and J. Zittartz, *Physica A* 295, 507–525 (2001).
34. S. Gopal and T. R. Smith, in M. M. Fischer, P. Nijkamp, and Y. Y. Papageorgiou (eds.) *Spatial Choices and Processes* (North-Holland, Amsterdam, 1990), pp. 169–200.
35. C. W. Reynolds, in D. Cliff, P. Husbands, J.-A. Meyer, and S. Wilson (eds.) *From Animals to Animats 3: Proceedings of the Third International Conference on Simulation of Adaptive Behavior* (MIT Press, Cambridge, Massachusetts, 1994), pp. 402–410.

36. D. Helbing, *Behavioral Science* 37, 190–214 (1992).
37. D. Helbing, P. Molnár, I. Farkas, and K. Bolay, *Environment and Planning B* 28, 361–383 (2001).
38. J. Klockgether and H.-P. Schwefel, in D. G. Elliott (ed.) *Proceedings of the Eleventh Symposium on Engineering Aspects of Magnetohydrodynamics* (California Institute of Technology, Pasadena, CA, 1970), pp. 141–148.
39. D. Helbing, in G. Haag, U. Mueller, and K. G. Troitzsch (eds.) *Economic Evolution and Demographic Change. Formal Models in Social Sciences* (Springer, Berlin, 1992), pp. 330–348.
40. N. E. Miller, in J. McV. Hunt (ed.) *Personality and the behavior disorders*, Vol. 1, (Ronald, New York, 1944).
41. N. E. Miller, in S. Koch (ed.) *Psychology: A Study of Science*, Vol. 2 (McGraw Hill, New York, 1959).
42. K. Lewin, *Field Theory in Social Science* (Harper & Brothers, New York, 1951).
43. D. Helbing, *Journal of Mathematical Sociology* 19(3), 189–219 (1994).
44. S. Hoogendoorn and P. H. L. Bovy, *Optimal Control Applications and Methods* 24(3), 153–172 (2003).
45. A. Johansson, D. Helbing, and P. K. Shukla, *Advances in Complex Systems*, in print (2007).
46. T. I. Lakoba, D. J. Kaup, and N. M. Finkelstein, *Simulation* 81(5), 339–352 (2005).
47. A. Seyfried, B. Steffen, and T. Lippert, *Physica A* 368, 232–238 (2006).
48. J. Kerridge and T. Chamberlain, in N. Waldau, P. Gattermann, H. Knoflacher, and M. Schreckenberg (eds.) *Pedestrian and Evacuation Dynamics '05* (Springer, Berlin, 2005).
49. S. P. Hoogendoorn, W. Daamen, and P. H. L. Bovy, in *Proceedings of the 82nd Annual Meeting at the Transportation Research Board* (CDROM, Mira Digital Publishing, Washington D.C., 2003).
50. K. Teknomo, *Microscopic pedestrian flow characteristics: Development of an image processing data collection and simulation model* (PhD thesis, Tohoku University Japan, Sendai, 2002).
51. D. Helbing, A. Johansson and H. Z. Al-Abideen, *Physical Review E* 75, 046109 (2007).
52. L. P. Kadanoff, *Journal of Statistical Physics* 39, 267–283 (1985).
53. H. E. Stanley and N. Ostrowsky (Eds.), *On Growth and Form* (Martinus Nijhoff, Boston, 1986).
54. T. Arns, *Video films of pedestrian crowds* (Stuttgart, 1993).
55. H.-H. Stølum, *Nature* 271, 1710–1713 (1996).
56. I. Rodríguez-Iturbe and A. Rinaldo, *Fractal River Basins: Chance and Self-Organization* (Cambridge University, Cambridge, England, 1997).
57. D. Helbing, I. Farkas, and T. Vicsek, *Physical Review Letters* 84, 1240–1243 (2000).
58. T. Schelling, *Journal of Mathematical Sociology* 1, 143–186 (1971).
59. D. Helbing and T. Platkowski, *International Journal of Chaos Theory and Applications* 5(4), 47–62 (2000).
60. S. P. Hoogendoorn and W. Daamen, *Transpn. Sci.* 39(2), 147–159 (2005).
61. T. Kretz, A. Grünebohm, and M. Schreckenberg, *J. Stat. Mech.* P10014 (2006).
62. K. Ando, H. Oto and T. Aoki, *Railway Research Review* 45 (8), 8–13 (1988).
63. K. H. Drager, G. Løvås, J. Wiklund, H. Soma, D. Duong, A. Violas, and V. Lanèrès, in the *Proceedings of the 1992 Emergency Management and Engineering Conference*, pp. 101–108 (Society for Computer Simulation, Orlando, Florida, 1992).
64. M. Ebihara, A. Ohtsuki, and H. Iwaki, *Microcomputers in Civil Engineering* 7, 63–71 (1992).

65. N. Ketchell, S. Cole, D. M. Webber, C. A. Marriott, P. J. Stephens, I. R. Brearley, J. Fraser, J. Doheny, and J. Smart, in *Engineering for Crowd Safety*, pp. 361–370, R. A. Smith and J. F. Dickie (Eds.) (Elsevier, Amsterdam, 1993).
66. S. Okazaki and S. Matsushita, in *Engineering for Crowd Safety*, pp. 271–280, R. A. Smith and J. F. Dickie (Eds.) (Elsevier, Amsterdam, 1993).
67. G. K. Still, *New computer system can predict human behaviour response to building fires*, *Fire* 84, 40–41 (1993).
68. G. K. Still, *Crowd Dynamics* (Ph.D. thesis, University of Warwick, 2000).
69. P. A. Thompson and E. W. Marchant, *Modelling techniques for evacuation*, in *Engineering for Crowd Safety*, pp. 259–269, R. A. Smith and J. F. Dickie (Eds.) (Elsevier, Amsterdam, 1993).
70. G. G. Løvås, *On the importance of building evacuation system components*, *IEEE Transactions on Engineering Management* 45, 181–191 (1998).
71. H. W. Hamacher and S. A. Tjandra, in M. Schreckenberg and S. D. Sharma (eds.) *Pedestrian and Evacuation Dynamics* (Springer, Berlin, 2001), pp. 227–266.
72. D. Elliott and D. Smith, *Football stadia disasters in the United Kingdom: Learning from tragedy?*, *Industrial & Environmental Crisis Quarterly* 7(3), 205–229 (1993).
73. B. D. Jacobs and P. 't Hart, in *Hazard Management and Emergency Planning*, Chap. 10, D. J. Parker and J. W. Handmer (Eds.) (James & James Science, London, 1992).
74. D. Canter (Ed.), *Fires and Human Behaviour*, (David Fulton, London, 1990).
75. A. Mintz, *The Journal of Abnormal and Normal Social Psychology* 46, 150–159 (1951).
76. J. P. Keating, *Fire Journal*, 57–61+147 (May/1982).
77. D. L. Miller, *Introduction to Collective Behavior*, Fig. 3.3 and Chap. 9 (Wadsworth, Belmont, CA, 1985).
78. J. S. Coleman, *Foundations of Social Theory*, Chaps. 9 and 33 (Belknap, Cambridge, MA, 1990).
79. N. R. Johnson, *Panic at "The Who Concert Stampede": An empirical assessment*, *Social Problems* 34(4), 362–373 (1987).
80. G. LeBon, *The Crowd* (Viking, New York, 1960 [1895]).
81. E. Quarantelli, *Sociology and Social Research* 41, 187–194 (1957).
82. N. J. Smelser, *Theory of Collective Behavior*, (The Free Press, New York, 1963).
83. R. Brown, *Social Psychology* (The Free Press, New York, 1965).
84. R. H. Turner and L. M. Killian, *Collective Behavior* (Prentice Hall, Englewood Cliffs, NJ, 3rd ed., 1987).
85. J. L. Bryan, *Fire Journal*, 27–30+86–90 (Nov./1985).
86. R. Axelrod and W. D. Hamilton, *Science* 211, 1390–1396 (1981).
87. R. Axelrod and D. Dion, *Science* 242, 1385–1390 (1988).
88. N. S. Glance and B. A. Huberman, *Scientific American* 270, 76–81 (1994).
89. R. A. Smith and J. F. Dickie (Eds.), *Engineering for Crowd Safety* (Elsevier, Amsterdam, 1993).
90. H. H. Kelley, J. C. Condry Jr., A. E. Dahlke, and A. H. Hill, *Journal of Experimental Social Psychology* 1, 20–54 (1965).
91. D. Helbing, I. Farkas, and T. Vicsek, *Nature* 407, 487–490 (2000).
92. G. H. Ristow and H. J. Herrmann, *Physical Review E* 50, R5–R8 (1994).
93. D. E. Wolf and P. Grassberger (Eds.), *Friction, Arching, Contact Dynamics* (World Scientific, Singapore, 1997).
94. D. Helbing, A. Johansson, J. Mathiesen, M.H. Jensen and A. Hansen *Physical Review Letters* 97, 168001 (2006).

95. S. Ghashghaie, W. Breymann, J. Peinke, P. Talkner, and Y. Dodge, *Nature* **381**, 767–770 (1996).
 96. G. Peng and H. J. Herrmann, *Phys. Rev. E* **49**, R1796–R1799 (1994).
 97. F. Radjai and S. Roux, *Phys. Rev. Lett.* **89**, 064302 (2002).
 98. K. R. Sreenivasan, *Nature* **344**, 192–193 (1990).
 99. M. E. Cates, J. P. Wittmer, J.-P. Bouchaud, and P. Claudin, *Phys. Rev. Lett.* **81**, 1841–1844 (1998).
 100. P. Bak, K. Christensen, L. Danon, and T. Scanlon, *Phys. Rev. Lett.* **88**, 178501 (2002).
 101. P. A. Johnson and X. Jia, *Nature* **437**, 871–874 (2005).
 102. J. J. Fruin, in R. A. Smith and J. F. Dickie (eds.) *Engineering for Crowd Safety*, (Elsevier, Amsterdam, 1993), pp. 99–108.
 103. T. Baeck, *Evolutionary Algorithms in Theory and Practice* (Oxford University Press, New York, 1996).
 104. A. Johansson and D. Helbing, in N. Waldau, P. Gattermann, H. Knoflacher, and M. Schreckenberg (eds.) *Pedestrian and Evacuation Dynamics 2005*, (Springer-Verlag, Berlin, 2007), pp. 267–272.
- Books and Reviews**
105. G. Le Bon, *The Crowd* (Dover, 2002; 1st ed. 1895).
 106. P. R. Decicco (ed.) *Evacuation from Fires* (Baywood, 2001).
 107. E. R. Galea (ed.), *Pedestrian and Evacuation Dynamics 2003* (CMS Press, London, 2003).
 108. D. Helbing, P. Molnár, I. Farkas, and K. Bolay (2001) Self-organizing pedestrian movement. *Environment and Planning B* 28, 361–383.
 109. D. Helbing (2001) Traffic and related self-driven many-particle systems. *Reviews of Modern Physics* 73, 1067–1141.
 110. D. Helbing, L. Buzna, A. Johansson, and T. Werner (2005) Self-organized pedestrian crowd dynamics: Experiments, simulations, and design solutions. *Transportation Science* 39(1), 1–24.
 111. V. M. Predtechenskii and A. I. Milinskii, *Planning for Foot Traffic Flow in Buildings* (Amerind, New Delhi, 1978).
 112. M. Schreckenberg and S. D. Sharma (eds.) *Pedestrian and Evacuation Dynamics* (Springer, Berlin, 2002).
 113. R. A. Smith and J. F. Dickie (Eds.), *Engineering for Crowd Safety* (Elsevier, Amsterdam, 1993).
 114. G. K. Still, *Crowd Dynamics* Ph.D. thesis (University of Warwick, 2000).
 115. J. Surowiecki, *The Wisdom of Crowds* (Anchor, 2005).
 116. N. Waldau, P. Gattermann, and H. Knoflacher (eds.), *Pedestrian and Evacuation Dynamics 2005* (Springer, 2006).
 117. J. Tubbs and B. Meacham, *Egress Design Solutions: A Guide to Evacuation and Crowd Management Planning* (Wiley, 2007).
 118. U. Weidmann, *Transporttechnik der Fußgänger* (Schriftenreihe des Institut für Verkehrsplanung, Transporttechnik, Straßen- und Eisenbahnbau **90**, ETH Zürich, 1993).